Cyclooxygenase-2-Mediated Metabolism of Arachidonic Acid to 15-Oxo-eicosatetraenoic Acid by Rat Intestinal Epithelial Cells

ARTICLE *in* CHEMICAL RESEARCH IN TOXICOLOGY · DECEMBER 2007

Impact Factor: 3.53 · DOI: 10.1021/tx700130p · Source: PubMed

6 AUTHORS, INCLUDING:

Seon Hwa Lee
Tohoku University
76 PUBLICATIONS **2,465** CITATIONS
SEE PROFILE

Kannan Rangiah
Centre for Cellular and Molecular Platforms
14 PUBLICATIONS **239** CITATIONS
SEE PROFILE

Raymond N DuBois
Arizona State University
320 PUBLICATIONS **34,162** CITATIONS
SEE PROFILE

Ian A Blair
University of Pennsylvania
428 PUBLICATIONS **12,435** CITATIONS
SEE PROFILE

Cyclooxygenase-2-Mediated Metabolism of Arachidonic Acid to 15-Oxo-eicosatetraenoic Acid by Rat Intestinal Epithelial Cells

Seon Hwa Lee,[†] Kannan Rangiah,[†] Michelle V. Williams,[†] Angela Y. Wehr,[†] Raymond N. DuBois,[‡] and Ian A. Blair*[,†]

Centers for Cancer Pharmacology and Excellence in Environmental Toxicology, University of Pennsylvania, 854 BRB II/III, 421 Curie Boulevard, Philadelphia, Pennsylvania 19104-6160, and Department of Medicine, Vanderbilt-Ingram Cancer Center, Vanderbilt University Medical Center, 698 Preston Research Building, Nashville, Tennessee 37232-6838

Received April 25, 2007

Rat intestinal epithelial cells that permanently express the cyclooxygenase-2 (COX-2) gene (RIES cells) were used to investigate COX-2-mediated arachidonic acid (AA) metabolism. A targeted chiral lipidomics approach was employed to quantify AA metabolites that were secreted by the cells into the culture media. When intact RIES cells were treated with calcium ionophore A-23187 (1 μM) for 1 h, 11-(*R*)-hydroxyeicosatetraenoic acid (HETE) was the most abundant metabolite, followed by prostaglandin (PG) E_2, 15-(*S*)-HETE, 15-oxo-eicosatetraenoic acid (ETE), and 15-(*R*)-HETE. Incubation for a further 23 h after the calcium ionophore was removed resulted in a substantial increase in PGE_2 concentrations while HETE and 15-oxo-ETE concentrations decreased to almost undetectable levels. A similar metabolic profile was observed when RIES cells were treated with increasing concentrations of AA for 24 h. Incubation of the RIES cells with 10 μM AA revealed that maximal concentrations of 11-(*R*)-HETE, 15-(*S*)-HETE, and 15-oxo-ETE occurred after 10 min of incubation when the 15-(*S*)-HETE concentrations were approximately twice that of PGE_2. There was a gradual decrease in the concentrations of HETE and 15-oxo-ETE over time, whereas PGE_2 concentrations increased steadily until they reached a maximum after 24 h of incubation. The ratio of PGE_2 to 15-(*S*)-HETE was then approximately 20:1. 15-(*S*)-HETE and 15-oxo-ETE concentrations declined in the cell media during prolonged incubations with pseudo-first-order rate constants of 0.0121 and 0.0073 min^{-1}, respectively. 15-(*S*)-HETE was shown to undergo metabolism primarily to 15-oxo-ETE, which was further metabolized to a glutathione (GSH) adduct. The GSH adduct of 15-oxo-ETE was further metabolized in the extracellular milieu to a cysteinylglycine adduct. Thus, we have established for the first time that 15-oxo-ETE can be formed biosynthetically from AA, that 15-(*S*)-HETE is its immediate precursor, and that 15-oxo-ETE forms a GSH adduct. For ionophore-A-23187-stimulated cells and at early time points for AA-stimulated cells, 11-(*R*)-HETE was the major eicosanoid to be secreted into the media. Adding increasing concentrations of AA to cells in culture made it possible to estimate with surprising accuracy endogenous eicosanoid production using regression analyses. Thus, after 24 h in the absence of added AA, 11-(*R*)-HETE and 15-(*R*)-HETE were estimated to be present at concentrations close to the detection limit of our very sensitive assay. These data further highlight the importance of endogenous COX-2-mediated lipid peroxidation and illustrate the necessity to monitor eicosanoid formation from endogenous stores of AA in cell culture experiments.

Introduction

Cyclooxygenase (COX)-[1] and lipoxygenase (LOX)-mediated pathways of arachidonic acid (AA) metabolism have been implicated as important mediators of carcinogenesis (*1, 2*). These pathways result in the formation of prostaglandins (PGs) as well as hydroperoxyeicosatetraenoic acids (HPETEs), hydroxyeicosatetraenoic acids (HETEs), and thromboxanes (*2, 3*). Inhibition of COXs by nonsteroidal anti-inflammatory drugs is known to be associated with a reduction in risk for colon and breast cancers (*4–6*). COX-2 expression is up-regulated in many tumors when it is absent from unaffected surrounding tissue (*7*). A number of studies have been conducted to determine how COX-2 mediates tumorigenesis. It has been suggested that COX-2 is involved in cellular proliferation, angiogenesis, resistance to apoptosis, enhancing invasiveness, and modulation of immunosuppression (*8*). These biological activities are thought to result primarily through the formation of PGs such as PGE_2. We have also suggested that the bifunctional electrophile, 4-oxo-2(*E*)-nonenal, which arises from homolytic decomposition of COX-2-derived 15-HPETE (*9, 10*), may give rise to mutagenic DNA adducts (*11–13*) that are involved in tumorigenesis (*14*).

* To whom correspondence should be addressed. Fax: 215-573-9889. E-mail: ian@spirit.gcrc.upenn.edu.
[†] University of Pennsylvania.
[‡] Vanderbilt University Medical Center.

[1] Abbreviations: AA, arachidonic acid; BDL, below detection limit; CID, collision-induced dissociation; COX, cyclooxygenase; 'DIPE, diisopropylethylamine; FBS, fetal bovine serum; GSH, glutathione; GST, glutathione-*S*-transferase; 12-HETE; 12-hydroxy-5,8,10,14-(*Z,Z,E,Z*)-eicosatetraenoic acid; 15-HETE, 15-hydroxy-5,8,11,14-(*Z,Z,Z,E*)-eicosatetraenoic acid; HPETE, hydroperoxyeicosatetraenoic acid; 8-*iso*-$PGF_{2\alpha}$, 9α,11α,15-(*S*)-trihydroxy-(8β)-prosta-5*Z*,13*E*-dien-1-oic acid; LC, liquid chromatography; LOX, lipoxygenase; MH^+, protonated molecule; MRM, multiple reaction monitoring; NS-398, N-[2-cyclohexyloyl-4-nitrophenyl]methane-sulfonamide; 15-oxo-ETE, 15-oxo-5*Z*,8*Z*,11*Z*,13*E*-eicosatetraenoic acid; PFB, pentafluorobenzyl; PG, prostaglandin; RIE, rat intestinal epithelial; RIES, RIE cells that express the COX-2 gene permanently; RPMI, Roswell Park Memorial Institute.

10.1021/tx700130p CCC: $37.00
Published on Web 10/02/2007

Previous studies of COX-2-mediated AA metabolism have been conducted primarily with recombinant enzymes (*15*), cells transiently transfected with COX-2 (*16*), or mitogen-treated cells where the enzyme activity is extremely high (*17*). There have been no comprehensive studies of cellular COX-2-mediated AA metabolism using cells that have a modest increase in COX-2 as compared with COX-1 activity such as the rat intestinal epithelial (RIE) cell line, which stably expresses COX-2 (RIES cells) developed by the DuBois group (*18*). We have shown that the COX-2 activity in the RIES cells (as measured by PGE_2 biosynthesis) is approximately five times greater than endogenous COX-1 activity (*9*). Therefore, the RIES cells provide a model system that closely relates to what is observed in epithelial cells isolated from colon tumors (*7, 18–20*). We have also shown that HPETE and HETE formation occurs primarily through COX-2-mediated AA metabolism in the RIES cells (*10*). In view of the potential for further metabolism of HPETEs and HETEs to bioactive molecules (*21–25*), a full characterization of eicosanoid biosynthesis was undertaken in the RIES cells. We reasoned that this would provide a more complete picture of the role that COX-2-mediated AA metabolism plays in tumorigenesis. Eicosanoid concentrations were determined by a targeted chiral lipidomics approach using stable isotope dilution liquid chromatography (LC)-electron capture atmospheric pressure chemical ionization/multiple reaction monitoring/mass spectrometry (APCI/MRM/MS) methodology (*26*). This made it possible to employ normal phase chiral chromatography to separate and quantify PGs and HETE isomers with extremely high sensitivity and specificity (*27, 28*).

Materials and Methods

Chemical and Materials. 9-Oxo-10*E*,12*Z*-octadecadienoic acid (9-oxo-ODE), 13-oxo-9*Z*,11*E*-octadecadienoic acid (13-oxo-ODE), 15-oxo-5*Z*,8*Z*,11*Z*,13*E*-eicosatetraenoic acid (15-oxo-ETE), 9-(*R*)-hydroxy-10*E*,12*Z*-octadecadienoic acid[9-(*R*)-HODE], 9-(*S*)-hydroxy-10*E*,12*Z*-octadecadienoic acid[9-(*S*)-HODE], 13-(*R*)-hydroxy-9*Z*,11*E*-octadecadienoic acid[13-(*R*)-HODE], 13-(*S*)-hydroxy-9*Z*,11*E*-octadecadienoic acid[13-(*S*)-HODE], 11-(*R*)-hydroxy-5*Z*,8*Z*,12*E*,14*Z*-eicosatetraenoic acid[11-(*R*)-HETE], 11-(*S*)-hydroxy-5*Z*,8*Z*,12*E*,14*Z*-eicosatetraenoic acid[11-(*S*)-HETE], 12-(*R*)-hydroxy-5*Z*,8*Z*,10*E*,14*Z*-eicosatetraenoic acid[12-(*R*)-HETE], 12-(*S*)-hydroxy-5*Z*,8*Z*,10*E*,14*Z*-eicosatetraenoic acid[12-(*S*)-HETE], 15-(*R*)-hydroxy-5*Z*,8*Z*,11*Z*,13*E*-eicosatetraenoic acid[15-(*R*)-HETE], 15-(*S*)-hydroxy-5*Z*,8*Z*,11*Z*,13*E*-eicosatetraenoic acid[15-(*S*)-HETE], 9-oxo-11α,15*S*-dihydroxy-prosta-5*Z*,13*E*-dien-1-oic acid (PGE_2), 9-oxo-11β,15*S*-dihydroxy-prosta-5*Z*,13*E*-dien-1-oic acid (11β-PGE_2), 9-oxo-11α,15*S*-dihydroxy-(8β)-prosta-5*Z*,13*E*-dien-1-oic acid (8-*iso*-PGE_2), 9α,15*S*-dihydroxy-11-oxo-prosta-5*Z*,13*E*-dien-1-oic acid (PGD_2), 9α,11α,15*S*-trihydroxy-prosta-5*Z*,13*E*-dien-1-oic acid ($PGF_{2\alpha}$), 9α,11β,15*S*-trihydroxy-prosta-5*Z*,13*E*-dien-1-oic acid (11β-PGF_2), 9α,11α,15*S*-trihydroxy-(8β)-prosta-5*Z*,13*E*-dien-1-oic acid (8-*iso*-$PGF_{2\alpha}$; *i*$PF_{2\alpha}$-III), 9-oxo-11α,15*S*-dihydroxy-prosta-5*Z*,13*E*-dien-1-oic-3,3,4,4-$^2H_4$ acid ([$^2H_4$]PGE_2), 9α,11α,15*S*-trihydroxy-prosta-5*Z*,13*E*-dien-1-oic-3,3,4,4-$^2H_4$ acid ([$^2H_4$]$PGF_{2\alpha}$),[$^2H_4$]-13-(*S*)-hydroxy-9*Z*,11*E*-octadecadienoic acid {[$^2H_4$]-13-(*S*)-HODE},[$^2H_8$]-15-(*S*)-hydroxy-5*Z*,8*Z*,11*Z*,13*E*-eicosatetraenoic acid {[$^2H_8$]-15-(*S*)-HETE}, and NS-398 (N-[2-cyclohexyloyl-4-nitrophenyl]methanesulfonamide) were purchased from Cayman Chemical Co. (Ann Arbor, MI). Diisopropylethylamine (DIPE), 2,3,4,5,6-pentafluorobenzyl bromide (PFB-Br), and equine glutathione-*S*-transferase (GST) were purchased from Sigma-Aldrich (St. Louis, MO). Roswell Park Memorial Institute (RPMI) cell culture media and fetal bovine serum (FBS) were supplied by Gibco (Grand Island, NY). HPLC grade hexane, methanol, and isopropanol were obtained from Fisher Scientific Co. (Fair Lawn, NJ). Gases were supplied by Airgas East Inc. (Allentown, PA).

MS and LC. A Finnigan TSQ Quantum Ultra AM mass spectrometer (Thermo Fisher, San Jose, CA) was used for targeted lipidomics profile with LC system 1 and for the analysis of glutathione (GSH) adducts in 15-oxo-ETE-treated RIES cells with LC system 3. Unit resolution was maintained for both parent and product ions for full-scan and MRM analyses. For targeted lipidomics profiling, the instrument was equipped with an APCI source and operated in the negative ion mode. Operating conditions were as follows: The vaporizer temperature was 450 °C, and the heated capillary temperature was 250 °C, with a discharge current of 30 μA applied to the corona needle. Nitrogen was used for the sheath gas, auxiliary gas, and ion sweep gas set at 25, 3, and 3 (in arbitrary units), respectively. Collision-induced dissociation (CID) was performed using argon as the collision gas at 1.5 mTorr in the second (rf-only) quadrupole. An additional dc offset voltage was applied to the region of the second multipole ion guide (Q_0) at 10 V to impart enough translational kinetic energy to the ions so that solvent adduct ions dissociated to form sample ions.

Targeted chiral LC-electron capture APCI/MRM/MS analysis was conducted using PFB derivatives of 24 lipids and eight heavy isotope analogue internal standards. Used were the following MRM transitions: 9- and 13-oxo-ODE-PFB, *m/z* 293 → 113 (collision energy, 21 eV); 15-oxo-ETE-PFB, *m/z* 317 → 273 (collision energy, 14 eV); 9-(*R*)- and 9-(*S*)-HODE-PFB, *m/z* 295 → 171 (collision energy, 18 eV); [$^2H_4$]-9-(*S*)-HODE-PFB, *m/z* 299 → 172 (collision energy, 18 eV); 13-(*R*)- and 13-(*S*)-HODE-PFB, *m/z* 295 → 195 (collision energy, 18 eV); [$^2H_4$]-13-(*S*)-HODE-PFB, *m/z* 299 → 198 (collision energy, 18 eV); 5-(*R*)- and 5-(*S*)-HETE-PFB, *m/z* 319 → 115 (collision energy, 15 eV); [$^2H_8$]-5-(*S*)-HETE-PFB, *m/z* 327 → 116 (collision energy, 15 eV); 8-(*R*)- and 8-(*S*)-HETE-PFB, *m/z* 319 → 155 (collision energy, 16 eV); 11-(*R*)- and 11-(*S*)-HETE-PFB, *m/z* 319 → 167 (collision energy, 16 eV); 12-(*R*)- and 12-(*S*)-HETE-PFB, *m/z* 319 → 179 (collision energy, 14 eV); [$^2H_8$]-12-(*S*)-HETE-PFB, *m/z* 327 → 184 (collision energy, 14 eV); 15-(*R*)- and 15-(*S*)-HETE-PFB, *m/z* 319 → 219 (collision energy, 13 eV); [$^2H_8$]-15-(*S*)-HETE-PFB, *m/z* 327 → 226 (collision energy, 13 eV); PGE_2-PFB, PGD_2-PFB, 11β-PGE_2-PFB, and 8-*iso*-PGE_2-PFB, *m/z* 351 → 271 (collision energy, 18 eV); [$^2H_4$]PGE_2-PFB and[$^2H_4$]PGD_2-PFB, *m/z* 355 → 275 (collision energy, 18 eV); 11β-PGF_2-PFB, $PGF_{2\alpha}$-PFB, and 8-*iso*-$PGF_{2\ \alpha}$-PFB, *m/z* 353 → 309 (collision energy, 18 eV); and [$^2H_4$]$PGF_{2\alpha}$-PFB, *m/z* 357 → 313 (collision energy, 18 eV).

For the analysis of sulfhydryl adducts formed in 15-oxo-ETE-treated RIES cells, the instrument was equipped with a heated electrospray ionization (ESI) source and operated in the positive ion mode. Operating conditions were as follows: The spray voltage was 3500 V, the vaporizer temperature was 300 °C, and the heated capillary temperature was 275 °C. Nitrogen was used for the sheath gas and auxiliary gas set at 35 and 10 (in arbitrary units), respectively. CID was performed using argon as the collision gas at 1.5 mTorr in the second (rf-only) quadrupole. An additional dc offset voltage was applied to the region of the second multipole ion guide (Q_0) at 5 V. The MRM transitions used were as follows: 15-oxo-ETE−GSH adducts, *m/z* 626 → 497 (collision energy, 20 eV); 15-oxo-ETE−cysteinylglycine adducts, *m/z* 497 → 479 (collision energy, 20 eV).

A Finnigan LCQ ion trap mass spectrometer (Thermo Fisher) equipped with an ESI source was used in positive ion mode with LC system 2 for LC-MS and MS^n analysis of the reaction between 15-oxo-ETE and GSH in the presence of GST. The operating conditions were as follows: heated capillary, 250 °C; spray voltage, +5 kV. Nitrogen was used as the sheath (60 psi) and auxiliary (5 units) gas. The capillary voltage was 12.5 V, and the tube lens offset was 15 V. Full scanning analyses were performed in the range of *m/z* 300–1500. CID experiments coupled with multiple tandem mass spectrometry (MS^n) employed helium as the collision gas. The relative collision energy was set at 50% of the maximum (1 V).

A Waters Alliance 2690 HPLC system (Waters Corp., Milford, MA) was used for LC systems 1–3. For the normal phase chiral LC-APCI/MS analysis, a Chiralpak AD-H column (250 mm × 4.6 mm i.d., 5 μm; Daicel Chemical Industries, Ltd., Tokyo, Japan) was employed with a flow rate of 1.0 mL/min. Solvent A was

hexane, and solvent B was methanol/isopropanol (1:1, v/v). Gradient system 1 was as follows: 2% B at 0 min, 2% B at 3 min, 3.6% B at 11 min, 8% B at 15 min, 8% B at 27 min, 50% B at 30 min, 50% B at 35 min, and 2% B at 37 min Separations were performed at 30 °C using a linear gradient. LC system 2 employed a Phenomenex Jupiter C18 column (250 mm × 4.6 mm i.d., 5 μm; Phenomenex, Torrance, CA). Solvent A was 5 mM ammonium acetate in water/0.01% TFA (v/v), and solvent B was 5 mM ammonium acetate in acetonitrile/0.01% TFA (v/v). Gradient system 2 was as follows: 3% B at 0 min, 3% B at 3 min, 30% B at 9 min, 45% B at 20 min, 80% B at 21 min, 80% B at 24 min, and 3% B at 25 min The flow rate was 1.0 mL/min with a split flow between the mass spectrometer and the Hitachi L4000 UV detector (Hitachi, San Jose, CA) set at 224 nm. LC system 3 employed a Zorbax Extend-C18 column (150 mm × 2.1 mm i.d., 3.5 μm; Agilent, Santa Clara, CA) with a flow rate of 0.25 mL/min. Solvent A was 5 mM ammonium acetate in water containing 0.01% trifluoroacetic acid (v/v), and solvent B was 5 mM ammonium acetate in acetonitrile containing 0.01% trifluoroacetic acid (v/v). Gradient system 3 was as follows: 5% B at 0 min, 5% B at 3 min, 30% B at 20 min, 40% B at 25 min, 40% B at 30 min, 80% B at 32 min, 80% B at 35 min, and 5% B at 37 min

LC-UV chromatography for analysis of 15-oxo-ETE in the cell culture medium was conducted using gradient system 4 on a Hitachi L-6200A Intelligent Pump equipped with a Hitachi L4000 UV detector (Hitachi) set at 279 nm. The separation employed a Zorbax RX-SIL column (250 mm × 4.6 mm i.d., 5 μm; Agilent). Isocratic elution was conducted with a solvent mixture of hexane and isopropanol (197:3) containing 0.1% acetic acid. The flow rate was 1 mL/min. The separation was performed at ambient temperature. A typical retention time of 15-oxo-ETE was 5.7 min

Targeted Lipidomics Profile of RIES Cell Culture Media after Calcium Ionophore A-23187 Incubations. RIES cells were cultured in RPMI supplemented with 10% FBS, 2 mM glutamine, 100000 units/L penicillin, and 100000 units/L streptomycin until almost confluent. The medium was removed and replaced with medium containing 0.1% FBS and calcium ionophore A-23187 (1 μM final concentration). Cells were then incubated for 0, 5, 10, 30, and 45 min and 1 h at 37 °C. At the end of each incubation, the medium containing calcium ionophore A-23187 was removed and replaced with medium containing only 0.1% FBS. Cells were then incubated for a further 23 h at 37 °C. A portion of cell culture medium (3 mL) was transferred into a glass tube after incubation. Tubes containing cell culture medium alone (3 mL) were spiked with the following amounts of authentic lipid standards: 20, 50, 100, 200, 500, 1000, and 2000 pg. A mixture of internal standards {[$^2H_8$]-5-(*S*)-HETE, [$^2H_8$]-12-(*S*)-HETE, [$^2H_8$]-15-(*S*)-HETE, [$^2H_4$]-9-(*S*)-HODE, [$^2H_4$]-13-(*S*)-HODE, [$^2H_4$]PGE_2, [$^2H_4$]PGD_2, and [$^2H_4$]$PGF_{2\alpha}$, 1 ng each} was added to each analytical sample and standard solution. The analytical samples and standard solutions were adjusted to pH 3 with 2.5 N hydrochloric acid. Lipids were extracted with diethyl ether (4 mL × 2), the organic layer was then evaporated to dryness under nitrogen, and the residue redissolved in 100 μL of acetonitrile was treated with 100 μL of PFB-Br in acetonitrile (1:19, v/v) followed by 100 μL of DIPE in acetonitrile (1:9, v/v). The solution was heated at 60 °C for 60 min, allowed to cool, evaporated to dryness under nitrogen at room temperature, and redissolved in 100 μL of hexane/ethanol (97:3, v/v). Analysis of the PFB derivatives by normal phase chiral LC-electron capture APCI/MRM/MS was conducted on a 20 μL aliquot of this solution using gradient 1. Calibration curves were obtained with a linear regression analysis of peak area ratios of analytes against internal standard. Concentrations of bioactive lipids in the medium were calculated by interpolation from the calculated regression lines.

Incubation of RIES Cells with Increasing Concentrations of AA. RIES cells were cultured in RPMI supplemented with 10% FBS, 2 mM glutamine, 100000 units/L penicillin, and 100000 units/L streptomycin until almost confluent. The medium was removed and replaced with medium containing 0.1% FBS and increasing concentrations of AA (0, 1, 5, 10, 50, and 100 μM final concentration). Cells were then incubated for 24 h at 37 °C. Quantitation of bioactive lipids from cell culture medium (3 mL) was performed as described above.

Time Course of Eicosanoid Formation by RIES Cells after Treatment with 10 μM AA. RIES cells were cultured in RPMI supplemented with 10% FBS, 2 mM glutamine, 100000 units/L penicillin, and 100000 units/L streptomycin until almost confluent. The medium was removed and replaced with medium containing 0.1% FBS and AA (10 μM final concentration). Cells were then incubated for 0, 1, 5, 10, 30, and 45 min and 1, 2, 4, and 24 h at 37 °C. Quantitation of bioactive lipids from cell culture medium (3 mL) was performed as described above.

Incubations of RIES Cells with Aspirin or NS-398. Cells were cultured in RPMI supplemented with 10% FBS, 2 mM glutamine, 100000 units/L penicillin, and 100000 units/L streptomycin until almost confluent. The medium was removed and replaced with medium containing 0.1% FBS and the nonselective COX inhibitor aspirin or the selective COX-2 inhibitor NS-398 (110 μM) (*29, 30*), as described previously (*9*). Cells were then incubated alone, with ionophore A23187, or with varying concentrations of AA as described above.

Incubation of RIES Cells with 15-(*S*)-HETE. RIES cells were cultured in RPMI supplemented with 10% FBS, 2 mM glutamine, 100000 units/L penicillin, and 100000 units/L streptomycin until almost confluent. The medium was removed and replaced with medium containing 0.1% FBS and 15-(*S*)-HETE (0.8 μM final concentration). Cells were then incubated for 0, 0.5, 1, 3, 12, and 24 h at 37 °C. Quantitation of bioactive lipids from cell culture medium (3 mL) was performed as described above.

Reaction of 15-Oxo-ETE with GSH in the Presence of GST. GSH (4 mM) was incubated with 15-oxo-ETE (1 mM) in 100 mM potassium phosphate buffer (200 μL) containing 1 mM EDTA (pH 6.5) in the presence of equine GST (200 units/mL). Reaction mixtures were incubated at 37 °C for 2 h and then filtered through an Amicon Ultra-4 5000 filter, and a 20 μL aliquot was analyzed by LC-MS/UV using gradient system 2.

Analysis of GSH Adducts in 15-Oxo-ETE-Treated RIES Cells. RIES cells were cultured in RPMI supplemented with 10% FBS, 2 mM glutamine, 100000 units/L penicillin, and 100000 units/L streptomycin until almost confluent. The medium was removed and replaced with medium containing 0.1% FBS and 15-oxo-ETE (40 μM final concentration). Cells were then incubated for 24 h at 37 °C. At each time point, the cells and cell culture medium were collected for LC-MS or LC-UV analysis. The cell culture medium was loaded on a solid phase extraction column (C_{18}, 3 mL), which was preconditioned with acetonitrile and water. After they were washed with 3 mL of water, GSH adducts were eluted with 6 mL of 50% acetonitrile in water (portion 1) and the remaining 15-oxo-ETE was then eluted with 6 mL of acetonitrile (portion 2). The solutions were evaporated to dryness under nitrogen. The portion 1 containing GSH adducts was redissolved in 100 μL of methanol, and the portion 2 containing 15-oxo-ETE was redissolved in 100 μL of hexane. The cells were washed with PBS, resuspended in 300 μL of PBS, lysed by sonication, and then filtered through an Amicon Ultra-4 5000 filter. The cell lysate flow-through and cell media portion 1 were each analyzed in duplicate by LC-MRM/MS using gradient system 3 on the Finnigan Quantum Ultra AM mass spectrometer. The cell media portion 2 was analyzed in duplicate by LC-UV using gradient system 4.

Results

Targeted Lipidomics Analysis of RIES Cell Media. LC-electron capture APCI/MRM/MS analysis of 24 targeted lipids from RIES cell supernatants treated with calcium ionophore A-23187 or AA revealed the presence of 15-oxo-ETE[retention time (rt), 8.4 min], 11-(*R*)-HETE (rt, 11.5 min), 15-(*R*)-HETE (rt, 12.8 min), 15-(*S*)-HETE (rt, 16.3 min), and PGE_2 (rt, 31.6 min). Extracted chromatograms for 15-oxo-ETE, 11-(*R*)-HETE, 11-(*S*)-HETE, 15-(*R*)-HETE, 15-(*S*)-HETE,[$^2H_8$]-15-(*S*)-HETE, PGE_2, and[$^2H_4$]-PGE_2 derived from LC-electron capture APCI/

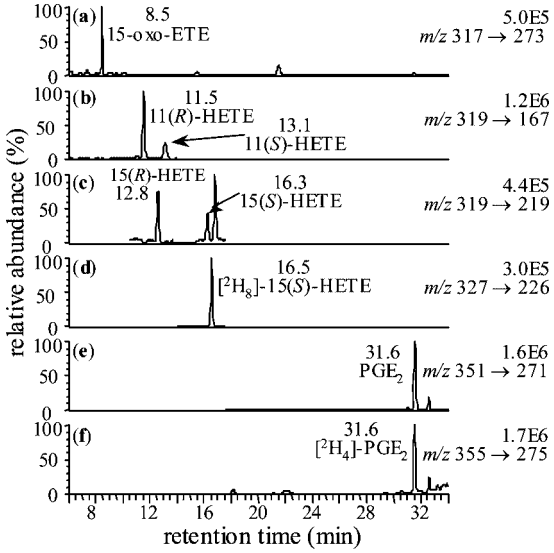

Figure 1. Targeted chiral lipidomics using LC-electron capture APCI/MS/MS for analysis of standard lipid PFB derivatives. MRM chromatograms are shown for (a) 15-oxo-ETE-PFB (*m/z* 317 → *m/z* 273), (b) 11-(*R*,*S*)-HETE-PFB (*m/z* 319 → *m/z* 167), (c) 15-(*R*,*S*)-HETE-PFB (*m/z* 319 → *m/z* 219), (d) [$^2H_8$]-15-(*S*)-HETE-PFB internal standard (*m/z* 327 → *m/z* 226), (e) PGE_2-PFB (*m/z* 351 → *m/z* 271), and (f) [$^2H_4$]-PGE_2-PFB internal standard (*m/z* 355 → *m/z* 275).

MRM/MS analysis of a standard mixture of 24 lipids and eight heavy isotope internal standards are shown in Figure 1. For quantitation of lipids, standard curves were constructed for all of the analytes in the range of 0.02–10.0 pmol/mL (1 mL = 10^5 cells). Typical regression lines for 15-oxo-ETE, 11-(*R*)-HETE, 15-(*R*)-HETE, 15-(*S*)-HETE, and PGE_2 were $y = 0.0029x + 0.0169$ ($r^2 = 0.9924$), $y = 0.0099x + 0.0459$ ($r^2 = 0.9989$), $y = 0.0015x + 0.0421$ ($r^2 = 0.9570$), $y = 0.0030x + 0.016$ ($r^2 = 0.9915$), and $y = 0.0026x + 0.0044$ ($r^2 = 0.9988$), respectively. [$^2H_8$]-15-(*S*)-HETE was used as an internal standard for 15-oxo-ETE, 11-(*R*)-HETE, 15-(*R*)-HETE, and 15-(*S*)-HETE. The assay was validated by demonstrating for replicate quality control samples with a precision of better than ± 15% and accuracy between 85 and 115% on three separate days.

Targeted Lipidomics Analysis of Calcium Ionophore-Treated RIES Cells. 11-(*R*)-HETE was the major product at all time points (Figure 2). The next most abundant metabolite was PGE_2, followed by 15-(*S*)-HETE, 15-oxo-ETE, and 15-(*R*)-HETE. Maximum 11-(*R*)-HETE (2.94 ± 0.15 pmol/10^6 cells), 15-(*S*)-HETE (1.08 ± 0.07 pmol/10^6 cells), 15-oxo-ETE (0.84 ± 0.06 pmol/10^6 cells), and 15-(*R*)-HETE (0.59 ± 0.04 pmol/10^6 cells) concentrations were observed after 10 min of incubation (Figure 2). Their concentrations were slightly decreased as the incubation time progressed. The enantiomeric excess of 15-(*S*)-HETE over 15-(*R*)-HETE was a mean of 38.4 ± 12.7% over the 60 min incubation period. Maximum PGE_2 concentrations of 2.30 ± 0.14 pmol/10^6 cells were observed after 45 min of incubation. At the end of each incubation, the medium containing calcium ionophore A-23187 was removed and replaced with medium containing only 0.1% FBS. Cells were then incubated for a total of 24 h at 37 °C. The product profiles of all incubations showed that there was an increase in concentration of PGE_2 at 5.7 ± 0.25 pmol/10^6 cells. However, the concentrations of 15-(*R*)- and 15-(*S*)-HETE were reduced to 0.11 ± 0.01 and 0.29 ± 0.02 pmol/10^6 cells, respectively. The concentrations of 15-oxo-ETE and 11-(*R*)-HETE were below the detection limit (BDL).

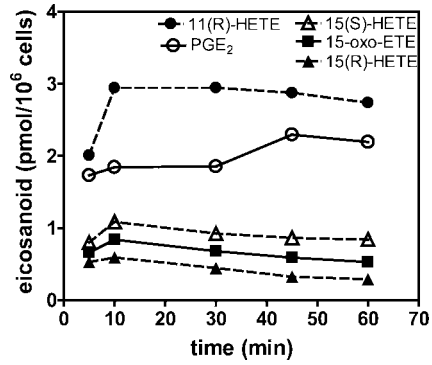

Figure 2. Amounts of 15-oxo-ETE, 11-(*R*)-HETE, 15-(*S*)-HETE, 15-(*R*)-HETE, and PGE_2 secreted by RIES cells into the media (pmol/10^6 cells) with treatment of calcium ionophore A-23187 (1 μM final concentration). Determinations were conducted in triplicate (means ± SEM) by stable isotope dilution LC-electron capture APCI/MRM/MS analysis of PFB derivatives.

Table 1. Eicosanoid Concentrations in the Media after Incubations of RIES Cells for 24 h in the Absence and Presence of AA (1–100 μM)[a]

AA concn (μM)	concentrations in (pmol/10^6 cells) after 24 h of incubation				
	11-(*R*)-HETE	PGE_2	15-(*S*)-HETE	15-oxo-ETE	15-(*R*)-HETE
0	BDL	0.94 ± 0.05	0.50 ± 0.05	BDL	BDL
1	0.44 ± 0.03	1.70 ± 0.06	0.69 ± 0.04	BDL	0.40 ± 0.02
5	0.53 ± 0.03	11.1 ± 0.64	0.72 ± 0.05	BDL	0.42 ± 0.03
10	0.92 ± 0.05	17.3 ± 0.86	1.01 ± 0.05	BDL	0.65 ± 0.04
50	1.98 ± 0.08	84.6 ± 3.21	2.58 ± 0.09	BDL	1.33 ± 0.04
100	9.41 ± 0.52	585 ± 15.1	14.3 ± 0.71	BDL	8.61 ± 0.43

[a] Detection limits: 11-(*R*)-, 15-(*S*)-, and 15-(*R*)-HETE = 0.20 pmol/10^6 cells (0.02 nM); 15-oxo-ETE = 0.50 pmol/10^6 cells (0.05 nM); and PGE_2 = 0.10 pmol/10^6 cells (0.01 nM).

Targeted Lipidomics Analysis of RIES Cells Treated with Increasing Concentrations of AA. PGE_2 was the major eicosanoid detected after incubating the RIES cells for 24 h (Table 1). It was also the major eicosanoid detected when exogenous AA was added to the cells for 24 h (Table 1). A linear dose-dependent increase in PGE_2 concentrations was observed with AA concentrations from 1 to 50 μM. PGE_2 concentrations went from 1.70 ± 0.06% pmol/10^6 cells with 1 μM AA to 84.6 ± 3.21 pmol/10^6 cells with 50 μM AA (Table 1). A linear regression of the dose response to AA ($y = 1.672x + 1.060$, $r^2 = 0.996$) predicted the endogenous concentration of PGE_2 to be 1.06 pmol/10^6 cells, which was only 13% higher than the 0.94 pmol/10^6 cells found experimentally (Table 1). When 100 μM AA was added to the cells, PGE_2 biosynthesis was much higher (585 pmol/10^6 cells) than predicted from the regression eq (168 pmol/10^6 cells). 15-(*S*)-HETE was the only HETE detected in the absence of exogenous AA. However, all of the HETEs could be detected when AA was added to the cells in concentrations as low as 1 μM. HETE concentrations increased in a linear dose-dependent manner up to 50 μM AA (Figure 3). A linear regression of the dose response to AA ($y = 0.570x + 0.596$, $r^2 = 0.996$) predicted the endogenous concentration of 15-(*S*)-HETE to be 0.60 pmol/10^6 cells, which was only 20% higher than the 0.50 pmol/10^6 cells found experimentally (Table 1). Linear regressions for 11-(*R*)-HETE ($y = 0.0318x + 0.3905$, $r^2 = 0.999$) and 15-(*R*)-HETE ($y = 0.019x + 0.389$, $r^2 = 0.986$), as shown in Figure 3, predicted endogenous concentrations of 0.39 pmol/10^6 cells for each of the two HETEs. These values were less than a factor of 2 above the limits of detection for 11-(*R*)-HETE and 15-(*R*)-HETE (0.20 pmol/10^6 cells), which explains why they were not detected

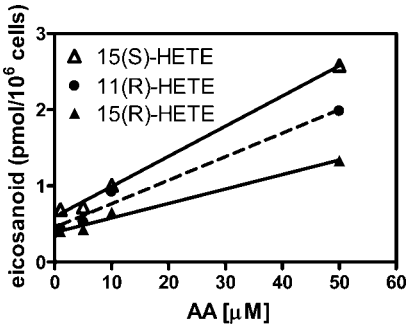

Figure 3. Regression analyses of HETE concentrations formed as a result of increasing concentrations of AA added to RIES cells. Equations of the regression lines are as follows: $y = 1.672x + 1.060$, $r^2 = 0.996$ (PGE_2, data not shown); $y = 0.570x + 0.596$, $r^2 = 0.996$ [15-(*S*)-HETE, open triangles]; $y = 0.0318x + 0.3905$, $r^2 = 0.999$ [11-(*R*)-HETE, closed circles]; and $y = 0.019x + 0.389$, $r^2 = 0.986$ [15-(*R*)-HETE, closed triangles].

Table 2. Ratios of Eicosanoid Concentrations in the Media after Incubations of RIES Cells for 24 h in the Absence and Presence of AA (1–100 μM)

AA concn (mM)	PGE_2/ 15-(*S*)-HETE	15-(*S*)-HETE/ 11-(*R*)-HETE	15-(*S*)-HETE/ 15-(*R*)-HETE	11-(*R*)-HETE/ 15-(*R*)-HETE
0	1.9	BDL	BDL	BDL
1	2.5	1.6	1.7	1.1
5	15.4	1.4	1.7	1.2
10	17.1	1.1	1.6	1.4
50	32.8	1.3	1.9	1.5
100	40.9	1.5	1.7	1.1
mean		1.4	1.7	1.3

unless AA was added to the cells. As was found for PGE_2, the biosynthesis of all three HETEs was much higher than predicted from the relevant regression equations when 100 μM AA was added to the cells. No 15-oxo-ETE was detected in the media after incubating RIES cells for 24 h in the presence or absence of AA (Table 1).

The ratio of PGE_2 to 15-(*S*)-HETE detected in the RIES cell incubation media was 1.9:1 after 24 h in the absence of AA (Table 2.). The ratio increased slightly to 2.5:1 when 1 μM AA was added to the incubation media. A dose-dependent increase in the ratio of PGE_2 to 15-(*S*)-HETE occurred with increasing concentrations of AA up to 100 μM, when the ratio was almost 41:1 (Table 2). In contrast, the relative ratios of 15-(*S*)-HETE to 11-(*R*)-HETE (1.4), 15-(*S*)-HETE to 15-(*R*)-HETE (1.7), and 11-(*R*)-HETE to 15-(*R*)-HETE (1.4) were essentially constant over the entire AA concentration range (Table 2). The mean enantiomeric excess of 15-(*S*)-HETE over 15-(*R*)-HETE was 26.3 ± 3.7%.

Targeted Lipidomics Analysis of RIES Cells Treated with 10 μM AA. Stable isotope dilution chiral LC-electron capture APCI/MS analysis of the cell media at all time points revealed the presence of 15-oxo-ETE, 11-(*R*)-HETE, 15-(*R*)-HETE, 15-(*S*)-HETE, and PGE_2 (Figures 4 and 5). At early incubation times, 11-(*R*)-HETE was the major product followed by 15-(*S*)-HETE, 15-(*R*)-HETE, 15-oxo-ETE, and PGE_2 (Figure 5). Maximum concentrations of HETEs and 15-oxo-ETE were observed after 10 min of incubation where the concentrations were 54.9 ± 2.4, 28.9 ± 1.4, 23.0 ± 1.4, 27.6 ± 1.4, and 12.5 ± 0.62 pmol/10^6 cells, respectively. There was then a gradual decrease in the concentrations of all of the HETEs and 15-oxo-ETE. At the 24 h time point, the concentrations of 11-(*R*)-HETE, 15-(*S*)-HETE, 15-(*R*)-HETE, and 15-oxo-ETE were 1.5 ± 0.04, 1.2 ± 0.04, 0.71 ± 0.02, and BDL pmol/10^6 cells, respectively. PGE_2 was the least abundant product until 30 min of incubation. As the incubation continued, PGE_2 formation increased steadily,

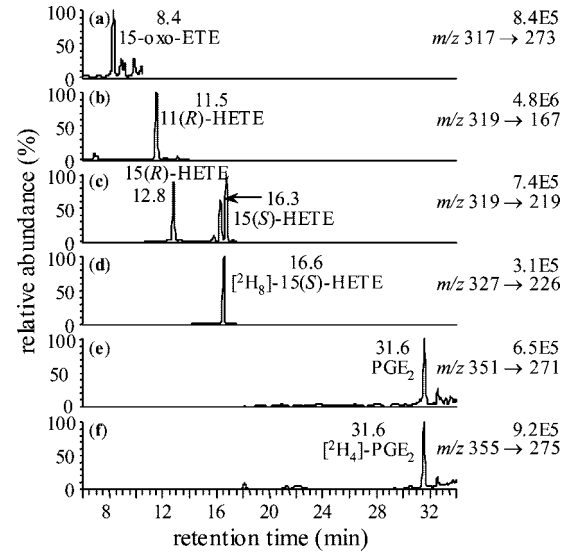

Figure 4. Targeted chiral lipidomics analysis of COX-2-derived eicosanoids from intact RIES cells treated with AA (10 μM final concentration) after 10 min Legends are as for Figure 1.

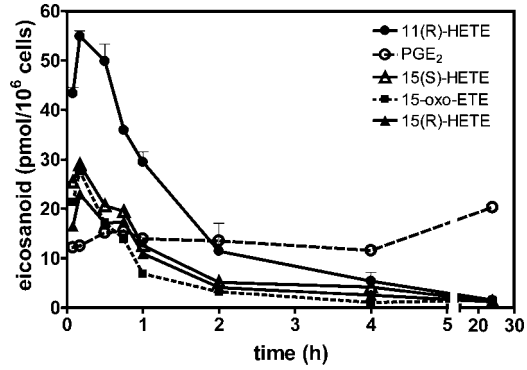

Figure 5. Amounts of 15-oxo-ETE, 11-(*R*)-HETE, 15-(*S*)-HETE, 15-(*R*)-HETE, and PGE_2 secreted by RIES cells into the media (pmol/10^6 cells) after addition of AA (10 μM final concentration). Determinations were conducted in triplicate (means ± SEM) by stable isotope dilution LC-electron capture APCI/MRM/MS analysis of PFB derivatives.

reaching maximum levels after 24 h, when the concentration was 20.3 ± 1.0 pmol/10^6 cells. PGE_2 became the most abundant metabolite after 2 h of incubation. Its concentration was approximately 13.5-fold higher than the HETEs and 15-oxo-ETE after 24 h of incubation.

Targeted Lipidomics Analysis of RIES Cells Treated with 15-(*S*)-HETE. 15-(*S*)-HETE concentrations declined from 0.8 μM to being close to the limit of detection after 3 h (Figure 6A). Conversely, there was an increase in the concentration of 15-oxo-ETE to a maximum of 0.07 (±0.02) μM or 0.7 (±0.2) nmol/10^6 cells at 1 h followed by a decline to undetectable levels after 12 h (Figure 6C).

Targeted Lipidomics Analysis of RIES Cells Treated with Aspirin or NS-398. PGE_2, HETE, and 15-oxo-ETE concentrations were reduced by >95% in the incubation media after stimulation with ionophore A23187 or AA (data not shown).

LC-MS and MS^n Analysis of the 15-Oxo-ETE−GSH Adduct. LC-MS/UV analysis of the products from the reaction between 15-oxo-ETE and GSH in the presence of GST revealed the presence of one major compound eluting at 17.5 min (data not shown). A MS full scan spectrum of this compound showed its protonated molecule (MH^+) at *m/z* 626. MS/MS analysis (Figure 7A) of MH^+ resulted in the formation of an intense

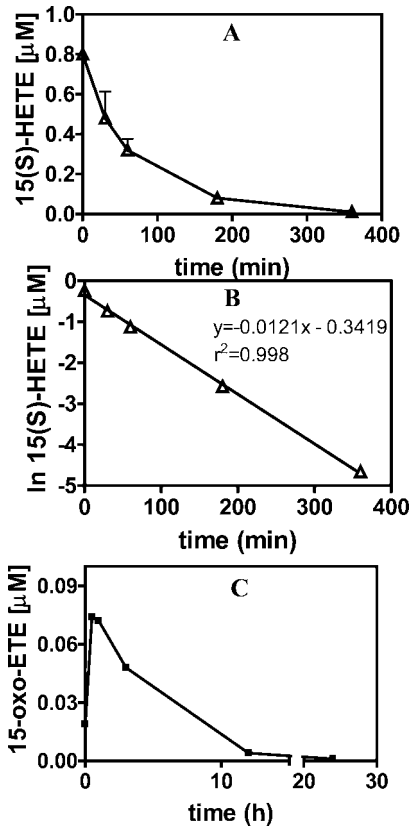

Figure 6. (A, B) Conversion of 15-(*S*)-HETE (0.8 μM) to 15-oxo-ETE by RIES cells. Concentrations in the cell media were determined in triplicate (means ± SEM) by stable isotope dilution LC-electron capture APCI/MRM/MS analysis of PFB derivatives. (A) Concentration−time plot of 15-(*S*)-HETE (μM) in cell culture media. (B) Kinetic plot of 15-(*S*)-HETE (μM) decline in the RIES cell media. (C) Concentration−time plot of 15-oxo-ETE (μM) in RIES cell culture media after the addition of 15-(*S*)-HETE (0.8 μM) determined in triplicate by LC-UV analysis.

product ion at *m/z* 497[a; $MH^+ - CO(CH_2)_2CH(NH_2)CO_2H + H$], which corresponded to the loss of the γ-glutamyl portion of the GSH adduct. This product ion has been observed in the MS/MS analysis of many other GSH adducts (*31*). MS (*3*) on *m/z* 497 gave rise to product ions at *m/z* 479 (a – H_2O), *m/z* 383[b; a – $CH_2CO(CH_2)_4CH_3$ – H], *m/z* 319[c; a – $SCH_2CH(NH)CONHCH_2COOH$ – 2H], *m/z* 301 (c – H_2O), *m/z* 283 (c – $2H_2O$), and *m/z* 179[d; $SCH_2CH(NH)CONHCH_2$-COOH + 3H] (Figure 7B). Product ions at *m/z* 319 (c) and *m/z* 179 (d) were formed from the cleavage of the carbon–sulfur bond, consistent with a cysteinylglycine adduct. The product ion at *m/z* 383 (b) corresponded precisely to the cleavage of the arachidonate carbon backbone between C-13 and C-14. This fragmentation pathway would be predicted if a carbon—sulfur thioether bond was present at C-13, which confirmed the 1,4-Michael addition of GSH to the α,β-unsaturated ketone in 15-oxo-ETE (Figure 7C).

Analysis of GSH and Cysteinylglycine Adducts in 15-Oxo-ETE-Treated RIES Cells. The concentration of 15-oxo-ETE in the extracellular milieu declined from 40 μM to being close to the limit of detection after 12 h. Loss of 15-oxo-ETE followed pseudofirst-order kinetics with a half-life of 95 min and a first-order rate constant (k) = 0.0073 min^{-1} (Figure 7D). 15-Oxo-ETE was quite stable in the cell culture medium for 24 h in the absence of the RIES cells. Intracellular and extracellular formation of 15-oxo-ETE–GSH and 15-oxo-ETE–cysteinylglycine adducts was monitored by LC-MRM/MS using gradient system 3. The 15-oxo-ETE–GSH adduct eluted at 25.4 min (Figure 8A), whereas the cysteinylglycine adduct eluted at 26.7 min (Figure 8B). Intracellular 15-oxo-ETE–GSH formation was maximal after 6 h of incubation and could not be detected after 24 h (Figure 8C). The GSH adduct was secreted into the media with a time course similar to that observed for its intracellular formation (Figure 8D). In contrast, the cysteinylglycine adduct was only detected in the incubation media. Its concentration in the incubation media increased over time to reach a maximum after 24 h of incubation (Figure 8D).

Discussion

RIES cells were grown to confluence as described previously (*9*) and incubated in media containing only 0.1% FBS. Serum was reduced to this low level because of the potential interference in LC-MS assays from endogenous HETEs, HODEs, and eicosanoids that are present in the FBS. Lipids and their heavy isotope internal standards were extracted from the media and converted to PFB derivatives to facilitate electron capture in the gas phase (*27, 28*). The derivatives were then subjected to a targeted lipidomics analysis (Figure 1). 11-(*R*)-HETE was the most abundant metabolite found in the media from ionophore A-23187-treated RIES cells (Figure 2). The next most abundant metabolite was PGE_2, followed by 15-(*S*)-HETE, 15-oxo-ETE, and 15-(*R*)-HETE. The ratio of PGE_2 to 15-(*S*)-HETE (2.9:1) in the ionophore-treated cells after 1 h (Figure 2) was similar to that observed in unstimulated cells (1.9:1) after 24 h in the present study (Table 2) and in our previous study (*10*). The enantiomeric excess of 15-(*S*)-HETE over 15-(*R*)-HETE was a mean of 38.4 ± 12.7% when cells were stimulated with ionophore A-23187 over 60 min (Figure 2).

Concentrations of HETEs and 15-oxo-ETE were maximal after 10 min of incubation with ionophore A-23187 and decreased slightly over the following 50 min (Figure 2). In contrast, PGE_2 concentrations were maximal after 45 min of incubation. The PGE_2 to 15-(*S*)-HETE ratio was 1.7:1 after 10 min of incubation with calcium ionophore and increased to 2.9:1 after 60 min PGE_2 became by far the major metabolite when media from the ionophore treatment were replaced with ionophore-free 0.1% FBS media and the incubation continued for a total of 24 h. In fact, 15-oxo-ETE and the HETEs could barely be detected after 24 h. These data suggested that 15-hydroxy-5,8,11,14-(*Z,Z,Z,E*)-eicosatetraenoic acids (15-HETEs) were being metabolized to 15-oxo-ETE (Scheme 1). COX-2-Mediated Metabolism of AA to PGE_2, HETEs, and 15-Oxo-ETE.), which then together with 11-(*R*)-HETE underwent further metabolism to eicosanoids that could not be detected in the targeted analysis.

When RIES cells were treated with increasing concentrations of AA for 24 h, PGE_2 was the major metabolite and its concentration increased in a dose-dependent manner. HETE and 15-oxo-ETE concentrations also increased in a dose-dependent manner, although they were much lower than PGE_2 (Table 1). The metabolite patterns at all AA concentrations were similar to those observed in 24 h incubations of RIES cells in calcium ionophore-free media after the initial 1 h treatment with calcium ionophore. This confirmed that 15-oxo-ETE and the HETEs were undergoing further metabolism in RIES cells during prolonged incubations. The PGE_2 to 15-(*S*)-HETE ratio increased substantially as the AA concentration increased. Without AA treatment, the ratio of PGE_2 to 15-(*S*)-HETE was 1.9:1, whereas the ratio was 17:1 at 10 μM AA and 41:1 at 100 μM AA (Table 2). In contrast, relative amounts of 11-(*R*)-HETE and 15-HETEs were constant from 1 to 100 μM AA and the ratio of 15-(*S*)-HETE to 15-(*R*)-HETE was also constant (Table 2).

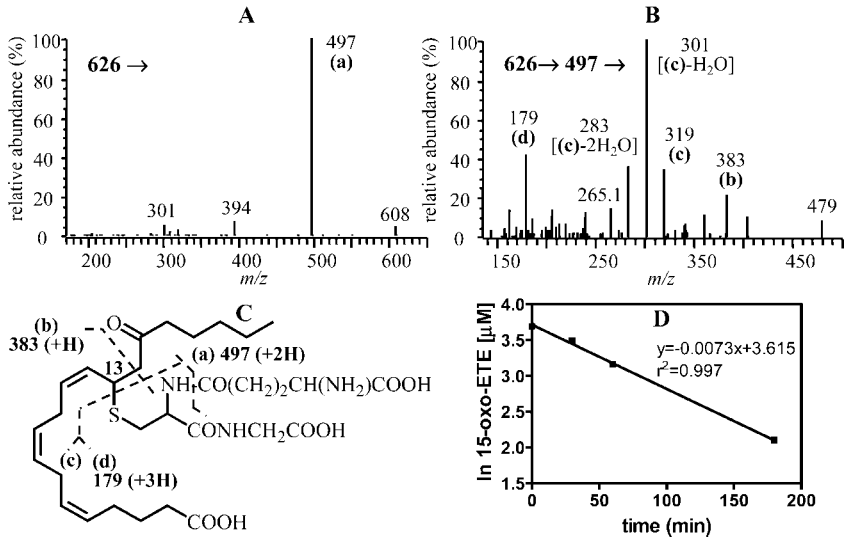

Figure 7. LC-MS^n analysis of 15-oxo-ETE−GSH. (A) MS^2 product ion spectrum. (B) MS^3 product ion spectrum. (C) Proposed structure of 15-oxo-ETE−GSH with indication of specific cleavages in multiple MS analyses. (D) Kinetic plot of 15-oxo-ETE (μM) decline in the RIES cell media.

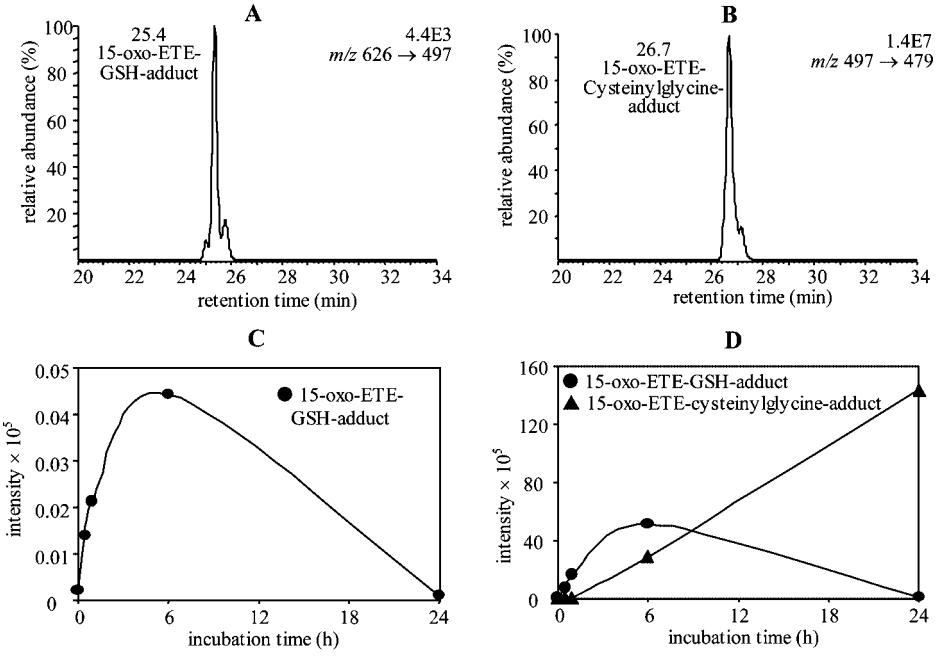

Figure 8. LC-MRM/MS analysis (using LC system 3) of GSH and cysteinylglycine adducts after incubation of RIES cells with 15-oxo-ETE (40 μM) for 24 h. (A) Intracellular formation of the 15-oxo-ETE−GSH adduct after 6 h of incubation showing MRM transition for *m/z* 626 → *m/z* 497. (B) Extracellular formation of the 15-oxo-cysteinylglycine adduct (*m/z* 497 → *m/z* 479) after 24 h of incubation. (C) Intracellular formation of the 15-oxo-ETE−GSH adduct over 24 h. (D) Extracellular formation of the 15-oxo-ETE−GSH adduct and the 15-oxo-cysteinylglycine adduct over 24 h.

At early time points, 11-(*R*)-HETE was the major product when RIES cells were incubated with 10 μM AA. Initially, 15-(*S*)-HETE was the next most abundant eicosanoid followed by 15-(*R*)-HETE, 15-oxo-ETE, and PGE_2 (Figure 5). However, 15-oxo-ETE concentrations were similar to 15-(*S*)- and 15-(*R*)-HETE after 10 min, which was when HETE and 15-oxo-ETE concentrations reached a maximum. At this time point, concentrations of 11-(*R*)-HETE were 4.4-fold higher and 15-(*S*)-HETE concentrations were 2-fold higher than PGE_2 (Figure 5). There was then a gradual decrease in HETE and 15-oxo-ETE concentrations over time so that after 2 h of incubation, PGE_2 was the most abundant eicosanoid. Concentrations of PGE_2 continued to increase steadily, reaching a maximum level after 24 h of incubation, when they were an order of magnitude higher than the HETEs and 15-oxo-ETE (Figure 5).

COX-2 expression (as determined by Western blot analysis) was maintained in the RIES cells for 24 h after the media containing 10% FBS had been replaced by media containing only 0.1% FBS (*9*). AA metabolite formation in the RIES media was reduced to undetectable levels by aspirin or NS-398, a COX-2 selective inhibitor (*29, 30*). This confirmed that the identified metabolites (Figures 2 and 5) arose primarily from COX-2-mediated metabolism of AA (*9*). AA is also an excellent substrate for human 15-LOX-1 (*32*) and 15-LOX-2 (*33–36*), which both produce exclusively 15-(*S*)-HPETE. The 15-(*S*)-HPETE is subsequently converted to 15-(*S*)-HETE by GSH-dependent peroxidases that are present in the cellular milieu (*37*). Rat leukocyte type 12/15-LOX and human 15-LOX-1 are homologous genes in the two different species (*38*). Therefore, it is conceivable that the RIES cells contained a 12/15-LOX

Scheme 1. COX-2-Mediated Metabolism of AA to PGE_2, HETEs, and 15-Oxo-ETE

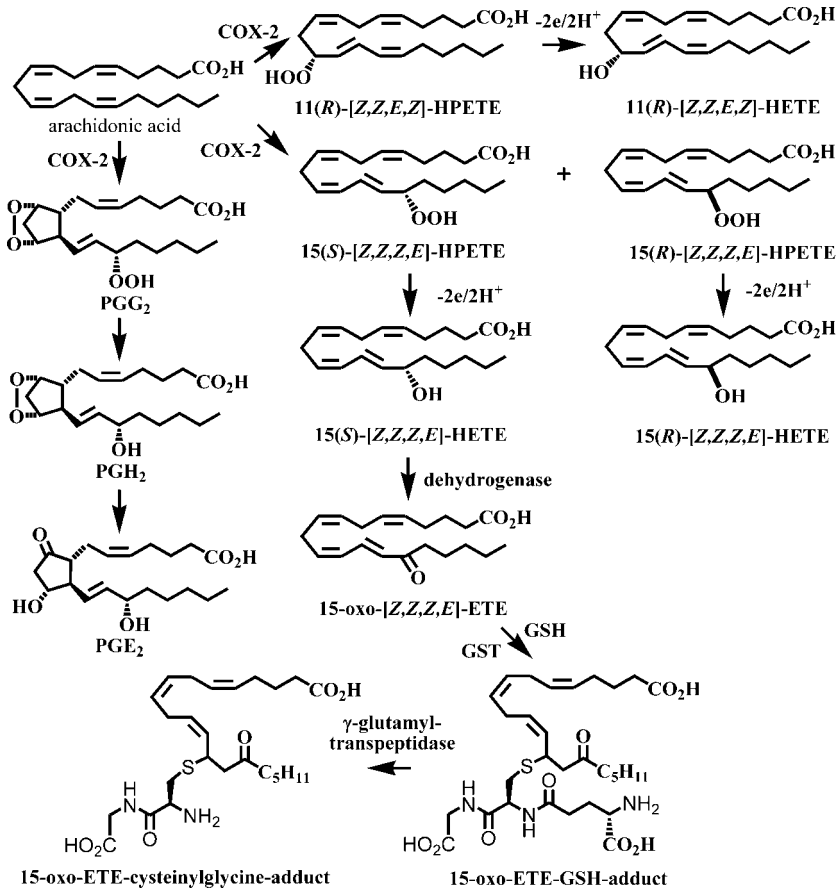

activity and that this was responsible for the AA-mediated formation of 15-(*S*)-HETE. However, previous studies by the Eling group have demonstrated that the RIES cells do not express any 12/15-LOX activity (*38*). Furthermore, they showed that the rat 12/15-LOX gene could be induced with sodium butyrate in wild-type RIE cells as demonstrated by the formation of 12-hydroxy-5,8,10,14-(*Z*,*Z*,*E*,*Z*)-eicosatetraenoic acid (12-HETE) and 15-HETE (*38*). No 12-HETE biosynthesis was observed in the present study, providing additional evidence that the cells did not possess any 12/15-LOX activity. In addition, reverse transcriptase polymerase chain reaction was employed to show that 15-LOX-2 mRNA was not expressed in the RIES cells (*9*). This eliminated the possibility that 15-(*S*)-HETE arose from 12/15-LOX expression in the RIES cells.

In previous studies with AA-treated intact cells, higher ratios of PGE_2 to 15-HETE formation were observed when COX-2 activity was strongly induced. For example, a study with cultured ovine tracheal epithelial cells in which COX-2 had been induced by growth factors reported that the ratio of 15-HETE to PGE_2 produced by adding 20 μM [^{3}H]AA was 1:15 (*17*). In microsomes from COS-7 cells transiently infected with recombinant COX-2, the ratio of 15-HETE to PGE_2 formation was 1:16 after a 30 min of incubation (*16*). However, the 15-HETE to PGE_2 ratio was increased by a factor of 2.5 (15-HETE to PGE_2 = 1:6) in freshly isolated ovine tracheal epithelial cells where there was an almost 4-fold lower capacity for PGE_2 biosynthesis as compared to the COX-2-induced cells (*17*). Furthermore, in human nasal polyp epithelial cells, which constitutively express COX-2, the ratio of 15-HETE to PGE_2 was close to 1:1 (*39*). In unstimulated intact RIES cells and ionophore A-23187-treated RIES cells, we determined that the 15-(*S*)-HETE to PGE_2 ratio was approximately 2:1 (*9*). This means that when cellular COX-2 levels are modestly induced, 15-HETE and PGE_2 are both major metabolites (Scheme 1). The use of ionophore or exogenously added AA and different incubation times can significantly affect HETE formation as well as the ratio of 15-HETE to PGE_2 (Figures 2 and 5).

15-Oxo-ETE can be readily prepared by hematin-mediated rearrangement of 15-(*S*)-HPETE (*40*) or by chemical synthesis (*41*). However, the present study is the first to show that 15-oxo-ETE can be formed through the cellular metabolism of AA. There have been a number of previous investigations on the metabolism of other HETE and HPETE regioisomers to oxo-ETEs. Thus, 5-(*S*)-HETE and 5-(*R*,*S*)-HPETE are metabolized to 5-oxo-ETE in intact neutrophils, monocytes, macrophages, and lymphocytes (*21–23, 25*). 12-Oxo-ETE was suggested to arise from a heme-mediated reaction with 12-(*S*)-HPETE in human platelet preparations (*40, 42*). In contrast, 12-(*R*)-HPETE is metabolized by ALOXE3 in skin to an isomer of hepoxilin A_3 and to 12-oxo-ETE (*43*).

Previous studies with linoleic acid- and AA-derived hydroperoxides and hydroxides (*21, 23, 25, 43–46*) raised the possibility that 15-oxo-ETE might arise from metabolism of both 15-HPETE and 15-HETE in the RIES cells. We have now unequivocally shown that 15-(*S*)-HETE undergoes conversion to 15-oxo-ETE (Figure 6A,C). The loss of 15-(*S*)-HETE followed pseudofirst-order kinetics with a half-life of 57 min and first-order rate constant (k) = 0.0121 min^{-1} (Figure 6B). There was a concomitant increase in the formation of 15-oxo-ETE, which underwent GST-mediated metabolism so that maximal concentrations were observed after 55 min in the media of RIES cells treated with 800 nM 15-(*S*)-HETE (Figure 6C). The 15-oxo-ETE was undetectable after 24 h of incubation. From the area under the concentration−time curve, the amount

of 15-oxo-ETE was estimated to be 438 nM, which corresponded to 55% conversion of 15-(*S*)-HETE to 15-oxo-ETE. The further GST-mediated metabolism of 15-oxo-ETE suggests that this may be in fact an underestimate. 15-Oxo-ETE was also formed when 15-(*S*)-HPETE was incubated with the RIES cells (data not shown). However, we cannot exclude the possibility that 15-oxo-ETE arose through the intermediate formation of 15-(*S*)-HETE (Scheme 1). The efficient formation of 15-oxo-ETE in the RIES cells suggests that there is a specific dehydrogenase present in the cells analogous the 5*S*-hydroxyeicosanoid dehydrogenase (5-HEDH) responsible for conversion of 5-(*S*)-HETE to 5-oxo-ETE in neutrophils, monocytes, and endothelial cells (*47–49*).

Interestingly, 5-oxo-ETE is 100 times more potent than 5-(*S*)-HETE at inducing neutrophil aggregation and migration (*35–37, 46, 50, 51*), whereas 15-oxo-ETE is essentially inactive (*46*). Conversely, 5-oxo- and 15-oxo-ETE have similar effects on cancer cell growth (*52*). Further metabolism of 5-oxo-ETE results in formation of a biologically active GSH adduct (*24, 53, 54*). Similarly, 13-HODE is converted to 13-oxo-ODE, which is subsequently converted to a GSH adduct (*54–58*). These previous studies suggested that 15-oxo-ETE might also form a GSH adduct. This would then explain why concentrations of 15-oxo-ETE declined on prolonged cellular incubations of RIES cells with AA (Figures 2 and 5) or with 15-(*S*)-HETE (Figure 6). To test this possibility, 15-oxo-ETE was treated with GSH in the presence of equine GST. A GSH adduct formed rapidly through 1,4-addition to the 15-oxo-moiety (Scheme 1). The 1,4-addion to the α,β-unsaturated ketone was consistent with the observed LC-MS^n spectrum (Figure 7A−C) and the lack of significant UV absorbance at 235 nm that would have been observed if 1,6-addition had occurred. The 1,4-addition of GSH to 15-oxo-ETE is similar to that reported for 5-oxo-ETE (*24*). When added to RIES cells, 15-oxo-ETE had a half-life of 95 min (Figure 7D), which was slightly longer than the 57 min half-life of 15-(*S*)-HETE. This was reflected in the lower first-order rate constant of 0.0073 min^{-1} observed for 15-oxo-ETE. LC-MRM/MS analysis revealed that the GSH adduct formed rapidly upon addition of 15-oxo-ETE to reach a maximal intracellular concentration after 6 h (Figure 8C). It also reached its maximum concentration in the cell media after 6 h (Figure 8D). Upon secretion into the media, the GSH adduct underwent hydrolysis to form a cysteinylglycine adduct, which was detected by LC-MRM/MS (Figure 8B). Cysteinylglycine adduct formation reached a maximum concentration in the cell media after 24 h of incubation (Figure 8D), but it was not detected in the cytosol. This suggests that hydrolysis of the GSH adduct is mediated by extracellular γ-glutamyltransferases as has been observed for many GSH adducts (*54*).

COX-1 and COX-2 both produce enantiomerically pure 11-(*R*)-HETE in vitro (*59, 60*). However, it was surprising that far more 11-(*R*)-HETE than PGE_2 was formed at early time points in both ionophore (Figure 2) and AA-treated (Figure 5) RIES cells. COX-2-mediated PG biosynthesis involves an initial oxygenation of AA at C-11 to an 11-(*R*)-peroxyl radical, which is followed by endoperoxide and cyclopentane ring formation. A second reaction with molecular oxygen at C-15, followed by a hydrogen abstraction, gives PGG_2 in which the hydroperoxy moiety is in the 15-(*S*) configuration (*61*). The formation of 11-(*R*)-HPETE is thought to arise from hydrogen abstraction by the 11-(*R*)-peroxyl radical when its rate of formation exceeds the rate of endoperoxide formation. Aspirin treatment of COX-2 causes acetylation of serine-516 in the human enzyme (*62*), which inhibits formation of both 11-(*R*)-HPETE and PGG_2 (*61*). However, 15-(*R*)-HPETE formation is actually increased by acetylation of COX-2. It has been suggested that this occurs because acetylated serine-516 in the human COX-2 (serine-530 in the mouse enzyme) forces a realignment of the ω-chain of AA. This unusual binding conformation appears to be responsible for oxygenation in the *R*-configuration (*60, 63–65*).

In view of the finding that 11-(*R*)-HETE was the major product at early time points in both ionophore A-23187- (Figure 2) and AA-treated (Figure 5) RIES cells, it was surprising that 11-oxo-ETE was not detected. Furthermore, 11-oxo-ETE has not been reported previously as a product of 11-(*R*)-HETE or 11-(*R*)-HPETE metabolism. Therefore, the decline in 11-(*R*)-HETE concentrations with time during the RIES cell incubations (Figure 5 and Table 1) might have resulted from metabolism through an alternative route such as the reductase pathway described previously for 12-(*S*)-HETE (*66*).

In summary, the addition of increasing concentrations of AA to cells in culture makes it possible to estimate endogenous eicosanoid production with surprising accuracy using regression analyses (Figure 3). Thus, the endogenous PGE_2 concentration in the RIES cell media was predicted with 13% accuracy and the lower 15-(*S*)-HETE concentration was predicted with 20% accuracy. It was also possible to estimate that endogenous 11-(*R*)-HETE and 15-(*S*)-HETE would be present at concentrations close to the detection limit of our very sensitive LC-MS assay. This explained our puzzling finding that 15-(*S*)-HETE and PGE_2 were the only COX-2-derived metabolites of endogenous AA metabolism that could be detected in incubations of RIES cells (Table 1) (*9*). In contrast, 11-(*R*)-HETE was the major eicosanoid to be secreted into the media for ionophore-A-23187-stimulated cells (Figure 2) and at earlier time points (<1 h) for AA-stimulated cells (Figure 5). Furthermore, under these conditions, both 15-(*R*)-HETE and 15-oxo-ETE could be detected in the media (Figures 2 and 5). The ratio of PGE_2 to 15-(*S*)-HETE increased dramatically from 1.9:1 (observed for endogenous biosynthesis) to a ratio 41:1 when 100 μM AA was added to the RIES cells (Table 2). However, the ratio between each of the HETEs remained remarkably constant over the entire concentration range of added AA (Table 2). The enantiomeric excess of 15-(*S*)-HETE to 15-(*R*)-HETE from COX-2-mediated metabolism of AA was slightly lower (26%) in the AA-stimulated cells when compared with cells stimulated with ionophore A-23187 (38%). These data further highlight the importance of endogenous COX-2-mediated lipid peroxidation and illustrate the necessity to monitor eicosanoid formation from endogenous stores of AA in cell culture experiments. Finally, the ability of 15-oxo-ETE to modulate cancer cell proliferation (*52*) suggests that the biological activity of this novel AA metabolite and its GSH and cysteinylglycine adducts warrants further investigation.

Acknowledgment. This work was supported by NIH Grants R01CA091016, R01CA095586, and P30ES013508.

References

(1) Sharma, R. A., Manson, M. M., Gescher, A., and Steward, W. P. (2001) Colorectal cancer chemoprevention: Biochemical targets and clinical development of promising agents. *Eur. J. Cancer 37*, 12–22.

(2) Jones, R., del-Alvarez, L. A., Alvarez, O. R., Broaddus, R., and Das, S. (2003) Arachidonic acid and colorectal carcinogenesis. *Mol. Cell. Biochem. 253*, 141–149.

(3) Chen, X., Sood, S., Yang, C. S., Li, N., and Sun, Z. (2006) Five-lipoxygenase pathway of arachidonic acid metabolism in carcinogenesis and cancer chemoprevention. *Curr. Cancer Drug Targets 6*, 613–622.

(4) Thun, M. J., Namboodiri, M. M., Calle, E. E., Flanders, W. D., and Heath, C. W., Jr. (1993) Aspirin use and risk of fatal cancer. *Cancer Res. 53*, 1322–1327.
(5) Thun, M. J., Henley, S. J., and Patrono, C. (2002) Nonsteroidal anti-inflammatory drugs as anticancer agents: Mechanistic, pharmacologic, and clinical issues. *J. Natl. Cancer Inst. 94*, 252–266.
(6) Davies, G. L. (2003) Cyclooxygenase-2 and chemoprevention of breast cancer. *J. Steroid Biochem. Mol. Biol. 86*, 495–499.
(7) Williams, C., Shattuck-Brandt, R. L., and Dubois, R. N. (1999) The role of COX-2 in intestinal cancer. *Ann. N. Y. Acad. Sci. 889*, 72–83.
(8) Wang, D., and Dubois, R. N. (2004) Cyclooxygenase-2: A potential target in breast cancer. *Semin. Oncol. 31*, 64–73.
(9) Lee, S. H., Williams, M. V., Dubois, R. N., and Blair, I. A. (2005) Cyclooxygenase-2-mediated DNA damage. *J. Biol. Chem. 280*, 28337–28346.
(10) Williams, M. V., Lee, S. H., Pollack, M., and Blair, I. A. (2006) Endogenous lipid hydroperoxide-mediated DNA-adduct formation in min mice. *J. Biol. Chem. 281*, 10127–10133.
(11) Rindgen, D., Nakajima, M., Wehrli, S., Xu, K., and Blair, I. A. (1999) Covalent modifications to 2′-deoxyguanosine by 4-oxo-2-nonenal, a novel product of lipid peroxidation. *Chem. Res. Toxicol. 12*, 1195–1204.
(12) Lee, S. H., and Blair, I. A. (2000) Characterization of 4-oxo-2-nonenal as a novel product of lipid peroxidation. *Chem. Res. Toxicol. 13*, 698–702.
(13) Pollack, M., Oe, T., Lee, S. H., Silva Elipe, M. V., Arison, B. H., and Blair, I. A. (2003) Characterization of 2′-deoxycytidine adducts derived from 4-oxo-2-nonenal, a novel lipid peroxidation product. *Chem. Res. Toxicol. 16*, 893–900.
(14) Pollack, M., Yang, I. Y., Kim, H. Y., Blair, I. A., and Moriya, M. (2006) Translesion DNA Synthesis across the heptanone−etheno-2′-deoxycytidine adduct in cells. *Chem. Res. Toxicol. 19*, 1074–1079.
(15) O'Neill, G. P., Mancini, J. A., Kargman, S., Yergey, J., Kwan, M. Y., Falgueyret, J. P., Abramovitz, M., Kennedy, B. P., Ouellet, M., and Cromlish, W. (1994) Overexpression of human prostaglandin G/H synthase-1 and -2 by recombinant vaccinia virus: inhibition by nonsteroidal anti-inflammatory drugs and biosynthesis of 15-hydroxyeicosatetraenoic acid. *Mol. Pharmacol. 45*, 245–254.
(16) Meade, E. A., Smith, W. L., and DeWitt, D. L. (1993) Expression of the murine prostaglandin (PGH) synthase-1 and PGH synthase-2 isozymes in cos-1 cells. *J. Lipid Mediators 6*, 119–129.
(17) Holtzman, M. J., Turk, J., and Shornick, L. P. (1992) Identification of a pharmacologically distinct prostaglandin H synthase in cultured epithelial cells. *J. Biol. Chem. 267*, 21438–21445.
(18) Tsujii, M., and Dubois, R. N. (1995) Alterations in cellular adhesion and apoptosis in epithelial cells overexpressing prostaglandin endoperoxide synthase 2. *Cell 83*, 493–501.
(19) Eberhart, C. E., Coffey, R. J., Radhika, A., Giardiello, F. M., Ferrenbach, S., and Dubois, R. N. (1994) Up-regulation of cyclooxygenase 2 gene expression in human colorectal adenomas and adenocarcinomas. *Gastroenterology 107*, 1183–1188.
(20) Sano, H., Kawahito, Y., Wilder, R. L., Hashiramoto, A., Mukai, S., Asai, K., Kimura, S., Kato, H., Kondo, M., and Hla, T. (1995) Expression of cyclooxygenase-1 and -2 in human colorectal cancer. *Cancer Res. 55*, 3785–3789.
(21) Powell, W. S., Gravelle, F., and Gravel, S. (1992) Metabolism of 5(S)-hydroxy-6,8,11,14-eicosatetraenoic acid and other 5(S)-hydroxyeicosanoids by a specific dehydrogenase in human polymorphonuclear leukocytes. *J. Biol. Chem. 267*, 19233–19241.
(22) Zhang, Y., Styhler, A., and Powell, W. S. (1996) Synthesis of 5-oxo-6,8,11,14-eicosatetraenoic acid by human monocytes and lymphocytes. *J. Leukocyte Biol. 59*, 847–854.
(23) Zarini, S., and Murphy, R. C. (2003) Biosynthesis of 5-oxo-6,8,11,14-eicosatetraenoic acid from 5-hydroperoxyeicosatetraenoic acid in the murine macrophage. *J. Biol. Chem. 278*, 11190–11196.
(24) Hevko, J. M., and Murphy, R. C. (2002) Formation of murine macrophage-derived 5-oxo-7-glutathionyl-8,11,14-eicosatrienoic acid (FOG7) is catalyzed by leukotriene C4 synthase. *J. Biol. Chem. 277*, 7037–7043.
(25) Powell, W. S., and Rokach, J. (2005) Biochemistry, biology and chemistry of the 5-lipoxygenase product 5-oxo-ETE. *Prog. Lipid Res. 44*, 154–183.
(26) Singh, G., Gutierrez, A., Xu, K., and Blair, I. A. (2000) Liquid chromatography/electron capture atmospheric pressure chemical ionization/mass spectrometry: analysis of pentafluorobenzyl derivatives of biomolecules and drugs in the attomole range. *Anal. Chem. 72*, 3007–3013.
(27) Lee, S. H., Williams, M. V., Dubois, R. N., and Blair, I. A. (2003) Targeted lipidomics using electron capture atmospheric pressure chemical ionization mass spectrometry. *Rapid Commun. Mass Spectrom. 17*, 2168–2176.
(28) Lee, S. H., Williams, M. V., and Blair, I. A. (2005) Targeted chiral lipidomics analysis. *Prostaglandins Other Lipid Mediators 77*, 141–157.
(29) O'Neill, G. P., Kennedy, B. P., Mancini, J. A., Kargman, S., Ouellet, M., Yergey, J., Falgueyret, J. P., Cromlish, W. A., Payette, P., and Chan, C. C. (1995) Selective inhibitors of COX-2. *Agents Actions Suppl. 46*, 159–168.
(30) Johnson, J. L., Wimsatt, J., Buckel, S. D., Dyer, R. D., and Maddipati, K. R. (1995) Purification and characterization of prostaglandin H synthase-2 from sheep placental cotyledons. *Arch. Biochem. Biophys. 324*, 26–34.
(31) Baillie, T. A., and Davis, M. R. (1993) Mass spectrometry in the analysis of glutathione conjugates. *Biol. Mass Spectrom. 22*, 319–325.
(32) Ikawa, H., Kamitani, H., Calvo, B. F., Foley, J. F., and Eling, T. E. (1999) Expression of 15-lipoxygenase-1 in human colorectal cancer. *Cancer Res. 59*, 360–366.
(33) Cashman, J. R., Lambert, C., and Sigal, E. (1988) Inhibition of human leukocyte 5-lipoxygenase by 15-HPETE and related eicosanoids. *Biochem. Biophys. Res. Commun. 155*, 38–44.
(34) Sigal, E., Grunberger, D., Cashman, J. R., Craik, C. S., Caughey, G. H., and Nadel, J. A. (1988) Arachidonate 15-lipoxygenase from human eosinophil-enriched leukocytes: Partial purification and properties. *Biochem. Biophys. Res. Commun. 150*, 376–383.
(35) Brash, A. R., Boeglin, W. E., and Chang, M. S. (1997) Discovery of a second 15S-lipoxygenase in humans. *Proc. Natl. Acad. Sci. U.S.A. 94*, 6148–6152.
(36) Kilty, I., Logan, A., and Vickers, P. J. (1999) Differential characteristics of human 15-lipoxygenase isozymes and a novel splice variant of 15S-lipoxygenase. *Eur. J. Biochem. 266*, 83–93.
(37) Kühn, H., and Borchert, A. (2002) Regulation of enzymatic lipid peroxidation: The interplay of peroxidizing and peroxide reducing enzymes. *Free Radical Biol. Med. 33*, 154–172.
(38) Kamitani, H., Geller, M., and Eling, T. (1999) The possible involvement of 15-lipoxygenase/leukocyte type 12-lipoxygenase in colorectal carcinogenesis. *Adv. Exp. Med. Biol. 469*, 593–598.
(39) Kowalski, M. L., Pawliczak, R., Wozniak, J., Siuda, K., Poniatowska, M., Iwaszkiewicz, J., Kornatowski, T., and Kaliner, M. A. (2000) Differential metabolism of arachidonic acid in nasal polyp epithelial cells cultured from aspirin-sensitive and aspirin-tolerant patients. *Am. J. Respir. Crit. Care Med. 161*, 391–398.
(40) Fruteau de Laclos, B., and Borgeat, P. (1988) Conditions for the formation of the oxo derivatives of arachidonic acid from platelet 12-lipoxygenase and soybean 15-lipoxygenase. *Biochim. Biophys. Acta 958*, 424–433.
(41) O'Flaherty, J. T., Cordes, J. F., Lee, S. L., Samuel, M., and Thomas, M. J. (1994) Chemical and biological characterization of oxo-eicosatetraenoic acids. *Biochim. Biophys. Acta 1201*, 505–515.
(42) Fruteau de Laclos, B., Maclouf, J., Poubelle, P., and Borgeat, P. (1987) Conversion of arachidonic acid into 12-oxo derivatives in human platelets. A pathway possibly involving the heme-catalysed transformation of 12-hydroperoxy-eicosatetraenoic acid. *Prostaglandins 33*, 315–337.
(43) Yu, Z., Schneider, C., Boeglin, W. E., Marnett, L. J., and Brash, A. R. (2003) The lipoxygenase gene ALOXE3 implicated in skin differentiation encodes a hydroperoxide isomerase. *Proc. Natl. Acad. Sci. U.S.A. 100*, 9162–9167.
(44) Bull, A. W., Earles, S. M., and Bronstein, J. C. (1991) Metabolism of oxidized linoleic acid: Distribution of activity for the enzymatic oxidation of 13-hydroxyoctadecadienoic acid to 13-oxooctadecadienoic acid in rat tissues. *Prostaglandins 41*, 43–50.
(45) Earles, S. M., Bronstein, J. C., Winner, D. L., and Bull, A. W. (1991) Metabolism of oxidized linoleic acid: Characterization of 13-hydroxyoctadecadienoic acid dehydrogenase activity from rat colonic tissue. *Biochim. Biophys. Acta 1081*, 174–180.
(46) O'Flaherty, J. T., Cordes, J., Redman, J., and Thomas, M. J. (1993) 5-Oxo-eicosatetraenoate, a potent human neutrophil stimulus. *Biochem. Biophys. Res. Commun. 192*, 129–134.
(47) Powell, W. S., Gravelle, F., Gravel, S., and Hashefi, M. (1993) Metabolism of 5(S)-hydroxyeicosanoids by a specific dehydrogenase in human neutrophils. *J. Lipid Mediators 6*, 361–368.
(48) Erlemann, K. R., Cossette, C., Grant, G. E., Lee, G. J., Patel, P., Rokach, J., and Powell, W. S. (2006) Regulation of 5-hydroxyeicosanoid dehydrogenase activity in monocytic cells. *Biochem. J.*
(49) Erlemann, K. R., Cossette, C., Gravel, S., Stamatiou, P. B., Lee, G. J., Rokach, J., and Powell, W. S. (2006) Metabolism of 5-hydroxy-6,8,11,14-eicosatetraenoic acid by human endothelial cells. *Biochem. Biophys. Res. Commun. 350*, 151–156.
(50) Powell, W. S., Gravel, S., MacLeod, R. J., Mills, E., and Hashefi, M. (1993) Stimulation of human neutrophils by 5-oxo-6,8,11,14-eicosatetraenoic acid by a mechanism independent of the leukotriene B4 receptor. *J. Biol. Chem. 268*, 9280–9286.

(51) O'Flaherty, J. T., Kuroki, M., Nixon, A. B., Wijkander, J., Yee, E., Lee, S. L., Smitherman, P. K., Wykle, R. L., and Daniel, L. W. (1996) 5-Oxo-eicosanoids and hematopoietic cytokines cooperate in stimulating neutrophil function and the mitogen-activated protein kinase pathway. *J. Biol. Chem. 271*, 17821–17828.

(52) O'Flaherty, J. T., Rogers, L. C., Paumi, C. M., Hantgan, R. R., Thomas, L. R., Clay, C. E., High, K., Chen, Y. Q., Willingham, M. C., Smitherman, P. K., Kute, T. E., Rao, A., Cramer, S. D., and Morrow, C. S. (2005) 5-Oxo-ETE analogs and the proliferation of cancer cells. *Biochim. Biophys. Acta 1736*, 228–236.

(53) Murphy, R. C., and Zarini, S. (2002) Glutathione adducts of oxyeicosanoids. *Prostaglandins Other Lipid Mediators 68–69*, 471–482.

(54) Blair, I. A. (2006) Endogenous glutathione adducts. *Curr. Drug Metab. 7*, 853–872.

(55) Bull, A. W., Bronstein, J. C., Earles, S. M., and Blackburn, M. L. (1996) Formation of adducts between 13-oxooctadecadienoic acid (13-OXO) and protein-derived thiols, in vivo and in vitro. *Life Sci. 58*, 2355–2365.

(56) Blackburn, M. L., Podgorski, I., and Bull, A. W. (1999) Specific protein targets of 13-oxooctadecadienoic acid (13-OXO) and export of the 13-OXO-glutathione conjugate in HT-29 cells. *Biochim. Biophys. Acta 1440*, 225–234.

(57) Podgorski, I., and Bull, A. W. (2001) Energy-dependent export of the 13-oxooctadecadienoic acid-glutathione conjugate from HT-29 cells and plasma membrane vesicles. *Biochim. Biophys. Acta 1533*, 55–65.

(58) Bull, A. W., Seeley, S. K., Geno, J., and Mannervik, B. (2002) Conjugation of the linoleic acid oxidation product, 13-oxooctadeca-9,11-dienoic acid, a bioactive endogenous substrate for mammalian glutathione transferase. *Biochim. Biophys. Acta 1571*, 77–82.

(59) Thuresson, E. D., Lakkides, K. M., and Smith, W. L. (2000) Different catalytically competent arrangements of arachidonic acid within the cyclooxygenase active site of prostaglandin endoperoxide H synthase-1 lead to the formation of different oxygenated products. *J. Biol. Chem. 275*, 8501–8507.

(60) Xiao, G., Tsai, A. L., Palmer, G., Boyar, W. C., Marshall, P. J., and Kulmacz, R. J. (1997) Analysis of hydroperoxide-induced tyrosyl radicals and lipoxygenase activity in aspirin-treated human prostaglandin H synthase-2. *Biochemistry 36*, 1836–1845.

(61) Schneider, C., Boeglin, W. E., Prusakiewicz, J. J., Rowlinson, S. W., Marnett, L. J., Samel, N., and Brash, A. R. (2002) Control of prostaglandin stereochemistry at the 15-carbon by cyclooxygenases-1 and -2. A critical role for serine 530 and valine 349. *J. Biol. Chem. 277*, 478–485.

(62) Smith, W. L., Garavito, R. M., and DeWitt, D. L. (1996) Prostaglandin endoperoxide H synthases (cyclooxygenases)-1 and -2. *J. Biol. Chem. 271*, 33157–33160.

(63) Rowlinson, S. W., Crews, B. C., Goodwin, D. C., Schneider, C., Gierse, J. K., and Marnett, L. J. (2000) Spatial requirements for 15-(*R*)-hydroxy-5*Z*,8*Z*,11*Z*,13*E*-eicosatetraenoic acid synthesis within the cyclooxygenase active site of murine COX-2. Why acetylated COX-1 does not synthesize 15-(*R*)-hete. *J. Biol. Chem. 275*, 6586–6591.

(64) Schneider, C., and Brash, A. R. (2000) Stereospecificity of hydrogen abstraction in the conversion of arachidonic acid to 15R-HETE by aspirin-treated cyclooxygenase-2. Implications for the alignment of substrate in the active site. *J. Biol. Chem. 275*, 4743–4746.

(65) Smith, W. L., Garavito, R. M., and DeWitt, D. L. (1996) Prostaglandin endoperoxide H synthases (cyclooxygenases)-1 and -2. *J. Biol. Chem. 271*, 33157–33160.

(66) Wainwright, S., Falck, J. R., Yadagiri, P., and Powell, W. S. (1990) Metabolism of 12(S)-hydroxy-5,8,10,14-eicosatetraenoic acid and other hydroxylated fatty acids by the reductase pathway in porcine polymorphonuclear leukocytes. *Biochemistry 29*, 10126–10135.

TX700130P